

CRITICAL FREQUENCIES OF THE IONOSPHERIC F_1 AND F_2 LAYERS DURING THE LAST FOUR SOLAR CYCLES: SUNSPOT GROUP TYPE DEPENDENCIES

ERDAL YİĞİT¹, ALI KILCIK², ANA GEORGINA ELIAS³, BURÇIN DÖNMEZ², ATILLA OZGUC⁴, VASYL YURCHSHYN^{5,6},
JEAN-PIERRE ROZELOT⁷,

ACCEPTED FOR PUBLICATION IN J. OF ATMOS. AND SOL-TERR. PHYS. Nov 29, 2017

ABSTRACT

The long term solar activity dependencies of ionospheric F_1 and F_2 regions' critical frequencies (f_0F_1 and f_0F_2) are analyzed for the last four solar cycles (1976–2015). We show that the ionospheric F_1 and F_2 regions have different solar activity dependencies in terms of the sunspot group (SG) numbers: F_1 region critical frequency (f_0F_1) peaks at the same time with the small SG numbers, while the f_0F_2 reaches its maximum at the same time with the large SG numbers, especially during the solar cycle 23. The observed differences in the sensitivity of ionospheric critical frequencies to sunspot group (SG) numbers provide a new insight into the solar activity effects on the ionosphere and space weather. While the F_1 layer is influenced by the slow solar wind, which is largely associated with small SGs, the ionospheric F_2 layer is more sensitive to Coronal Mass Ejections (CMEs) and fast solar winds, which are mainly produced by large SGs and coronal holes. The SG numbers maximize during of peak of the solar cycle and the number of coronal holes peaks during the sunspot declining phase. During solar minimum there are relatively less large SGs, hence reduced CME and flare activity. These results provide a new perspective for assessing how the different regions of the ionosphere respond to space weather effects.

1. INTRODUCTION

Sunspots are dark, cold and magnetically dense structures observed on the solar photosphere, the visible surface of Sun. They have been observed systematically since 1610 (Vaquero 2007; Clette et al. 2014). Generally, they are observed on the solar disc as groups and these groups have been classified according to their morphology, complexity, and evolution for about a century (Cortie 1901; McIntosh 1990). Using the number of observed groups and of individual spots the daily International sunspot number (or Zürich number) is calculated by (Wolf 1861):

$$R_z = k(10g + f), \quad (1)$$

where f is the number of individual spots, g is the number of observed sunspot groups, and k is a correction factor for each observatory. The sunspot number is the best known and the longest solar activity index and is a good proxy for the solar activity variations (Clette et al. 2014; Hathaway 2015). These variations can also be represented by other solar activity indicators, such as, sunspot areas (SSAs), sunspot group (SG) numbers, total solar irradiance (TSI), and 10.7 cm solar radio flux ($F_{10.7}$). The solar activity variations obtained from these indicators show small differences in time, depending on the description of indices and also the background physical

mechanisms. Hence we will limit ourselves to the analysis in time to SGs as the other indexes will follow more or less the same behavior.

R_z suggests that the daily sunspot number is directly related to the observed group and individual sunspot numbers, without taking into account group/sunspot properties. However, a robust result presented in the work by Kilcik et al. (2011a) indicates that the number of large SGs peaks about two years later than the small ones. It has also been found that large group numbers show a better correlation with the maximum speed of coronal mass ejections (CMEs) and geomagnetic indices (A_p and Dst) than the small ones for the solar cycle 23 (Kilkic et al. 2011b).

Solar activity variations strongly affect Earth's magnetosphere, ionosphere, and thermosphere. The terrestrial thermosphere-ionosphere system is extremely variable due primarily to the influence of lower atmospheric internal waves from below (Yigit and Medvedev 2015, and references therein) and geomagnetic and solar activity variations from above (e.g, Smithro and Sojka 2005; Yigit et al. 2016). Also, solar cycle variations may influence the propagation and dissipation of gravity waves in the thermosphere (Yigit and Medvedev 2010).

Extending from ~ 50 to ~ 1000 km, the ionosphere forms the partially ionized portion of the neutral upper atmosphere. A number of communication and navigation systems use the ionosphere in which radio signals are propagated and transmitted. Each ionospheric layer has a maximum frequency, known as critical frequency, at which radio waves can be transmitted through and be reflected back (for normal incidence) to Earth most efficiently. The ionosphere is transparent to the radio waves at frequencies higher than the critical frequency while waves will be reflected back to Earth at frequencies lower than the critical frequency (Elias et al. 2017).

Photoionization, which is responsible for the forma-

¹ Department of Physics and Astronomy, Space Weather Laboratory, George Mason University, Fairfax, Virginia, USA.

² Akdeniz University, Department of Space Sciences and Technologies, Turkey

³ Univ. Nacl. Tucuman, Fac. Ciencias Exactas and Tecnol., Dept. Fis., Argentina

⁴ Kandilli Observatory and Earthquake Research Institute, Bogazici University, Turkey

⁵ Big Bear Solar Observatory, Big Bear City, CA, USA

⁶ Korea Astronomy and Space Science Institute, Daejeon, Korea

⁷ Université de la Cote d'Azur, Grasse, France.

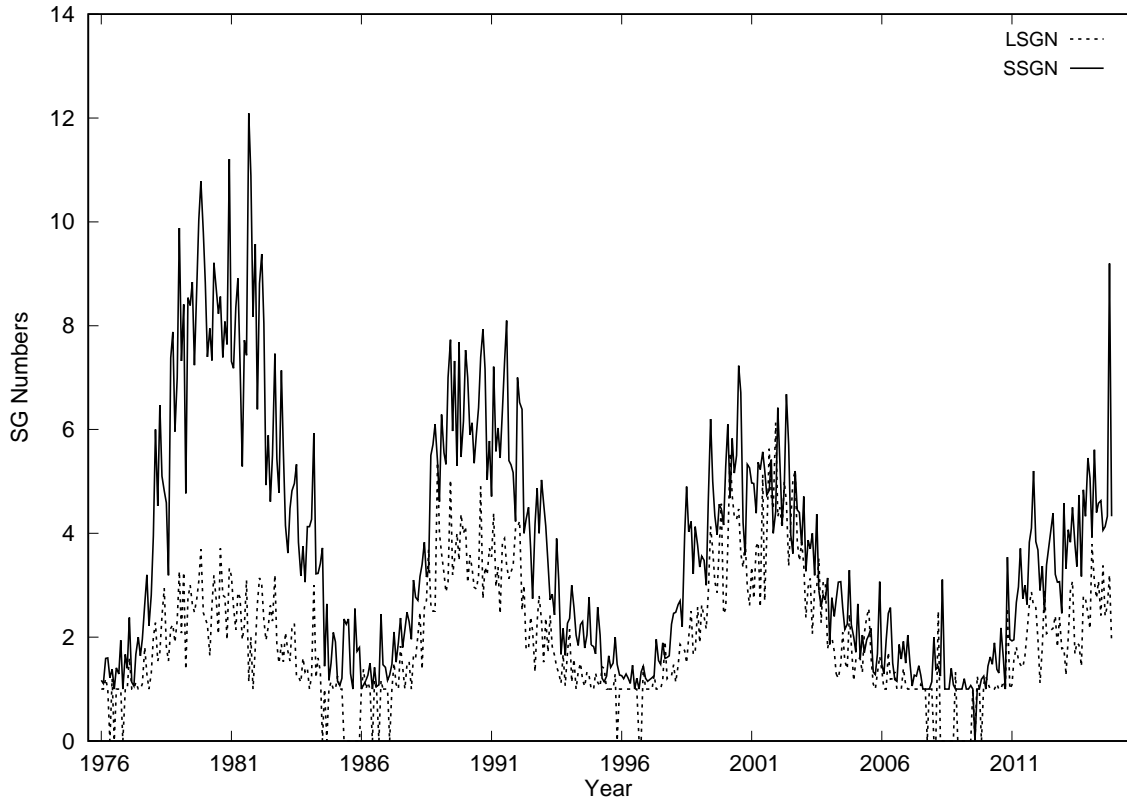


Figure 1. Monthly average large sunspot group number (LSGN) and small sunspot group number (SSGN) data for the last four solar cycles.

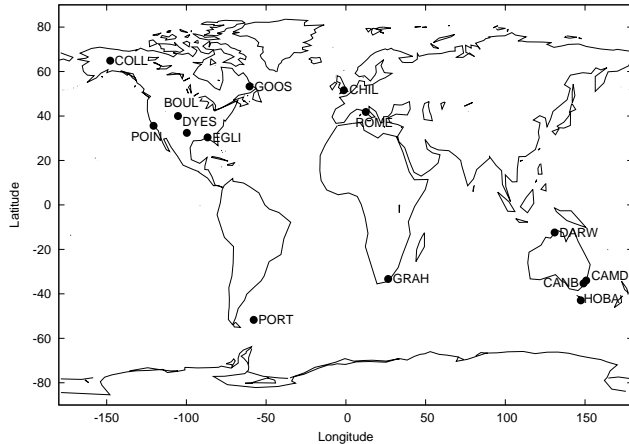


Figure 2. Global distribution of the ionospheric stations where the ionospheric critical frequencies (f_oF_1 , and f_oF_2) are observed.

tion ion-electron pairs, is dependent on the presence of the type of ionizable species, which can be influenced by other radiative loss process. The F_1 layer is primarily photochemically controlled. O^+ ions dominate as a consequence of the photoionization of neutral atomic oxygen, while it is lost by ion-molecule interchange with O_2 and N_2 . The F_2 region is rather dynamically controlled as a transition from chemical control to diffusive transport takes place. These dynamical processes include ambipolar diffusion, wind-induced drifts along the geomagnetic field, and wave effects. The peak ion content in the F-region occurs at the location where chemical and diffu-

sive effects are of equal importance, which leads to the formation of the F_2 layer.

Overall, the F_1 layer of the ionosphere exhibits dependence on the solar zenith angle, season, and geomagnetic activity. Therefore, it is more pronounced in the summer than in the winter, disappears during the night and sometimes during the winter days. On the contrary, the F_2 layer, where globally the largest amount of plasma is found, is a permanent feature of the ionosphere under all solar-terrestrial conditions.

Due to the importance of ionospheric critical frequencies for communication and their relationship with solar activity, it has been studied extensively by a number of authors (e.g., *Forbes et al. 2000*; *Kane 2006*; *Chakrabarty et al. 2014*, and references therein). Most of these studies compared the foF_2 critical frequency with solar activity variations in various time scales.

In this study, in order to better understand the response of the different ionospheric regions to solar variations, we examine the long-term temporal dependencies of ionospheric f_oF_1 and f_oF_2 critical frequencies to the SG numbers during the last three complete solar cycles (cycles 21, 22, and 23) and the ascending and maximum phases of solar cycle 24. Specifically, the temporal variations of f_oF_1 and f_oF_2 are compared with the variations of small and large sunspot groups. It is assumed that the connection is not due to the sunspots in themselves, but through the fluctuations of the activity that way generated. Thus we have emphasized this aspect, and in particular, by considering the double peaks which sometimes occurred in the solar activity not explained so far,

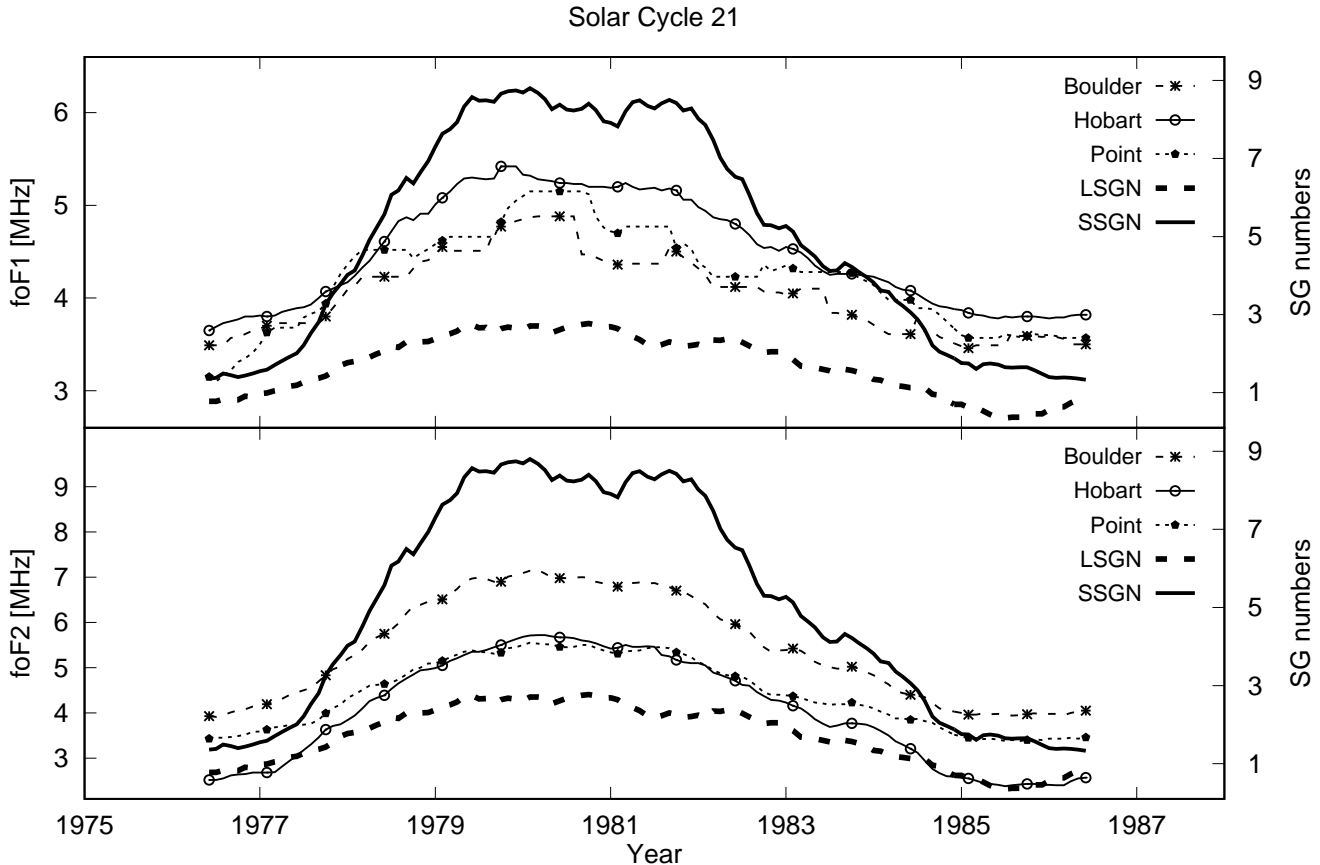


Figure 3. Temporal variations of the large (dashed line, LSSN) and small (solid line, SSSN) sunspot group numbers along with the variations of the ionospheric critical frequencies f_0F_1 (top panel) and f_0F_2 (bottom panel) in units of MHz during solar cycle 21. The different ionospheric stations are overplotted with different lines.

that may affect the behavior or corpuscular emissions (solar wind, CMEs, etc.) as well as the radiative effects.

The structure of the paper is as follows: Next Section (Section 2) briefly describes the data to be used in our analysis; Section 3 presents the results on the relationship between the ionospheric critical frequencies and the sunspot groups, and Section 4 presents the conclusions and briefly discusses their implications.

2. DATA

2.1. The Sunspot Group (SG) Number Data

The SG number data were downloaded from the National Geophysical Data Center (NGDC)⁸ for each recorded group during the observed day. The data were collected by the United States Air Force/Mount Wilson Observatory (USAF/MWL) since 1982 and the previous data are taken from Rome and Taipei Observatories. The USAF/MWL database also includes measurements from the Learmonth Solar Observatory, the Holloman Solar Observatory, and the San Vito Solar Observatory. We used the Learmonth station data as the principal data source for the last three cycles (since 1986), and gaps were filled with records from one of the other stations

listed above. Thus, a nearly continuous daily SG number data set was produced, according to the Modified Zurich Sunspot Classification, for both large (D,E,F) and small (A, B, C, H) groups. Due to the time coverage of USAF/MWL data set, the Rome observatory data are used as a reference data for cycle 21 and gaps in this data set were filled with Taipei observatory data. But, this data set still has many gaps compared to Learmonth data. As a final step, the monthly mean values for the large and small SGs were calculated. Temporal variation of the monthly large and small SGs is presented in Figure 1. To remove the short term fluctuations and reveal the long term trend 12-step running average smoothing was applied and used in the analysis.

2.2. Ionospheric Critical Frequencies Data

The ionospheric critical frequencies data for the selected stations are taken from Space Physics Interactive Data Resource, SPIDR⁹. To select these stations the main criteria was existence of continuous data for the investigated solar cycles. We used smoothed monthly median critical frequencies, f_0F_1 and f_0F_2 , recorded at 14 stations distributed over the globe (see Figure 2) within the period of 1976–2015, which cover three full solar cy-

⁸ <http://www.ngdc.noaa.gov/stp/space-weather/solar-data/solar-features/sunspot-regions/>

⁹ <http://spidr.ionosonde.net/spidr/>

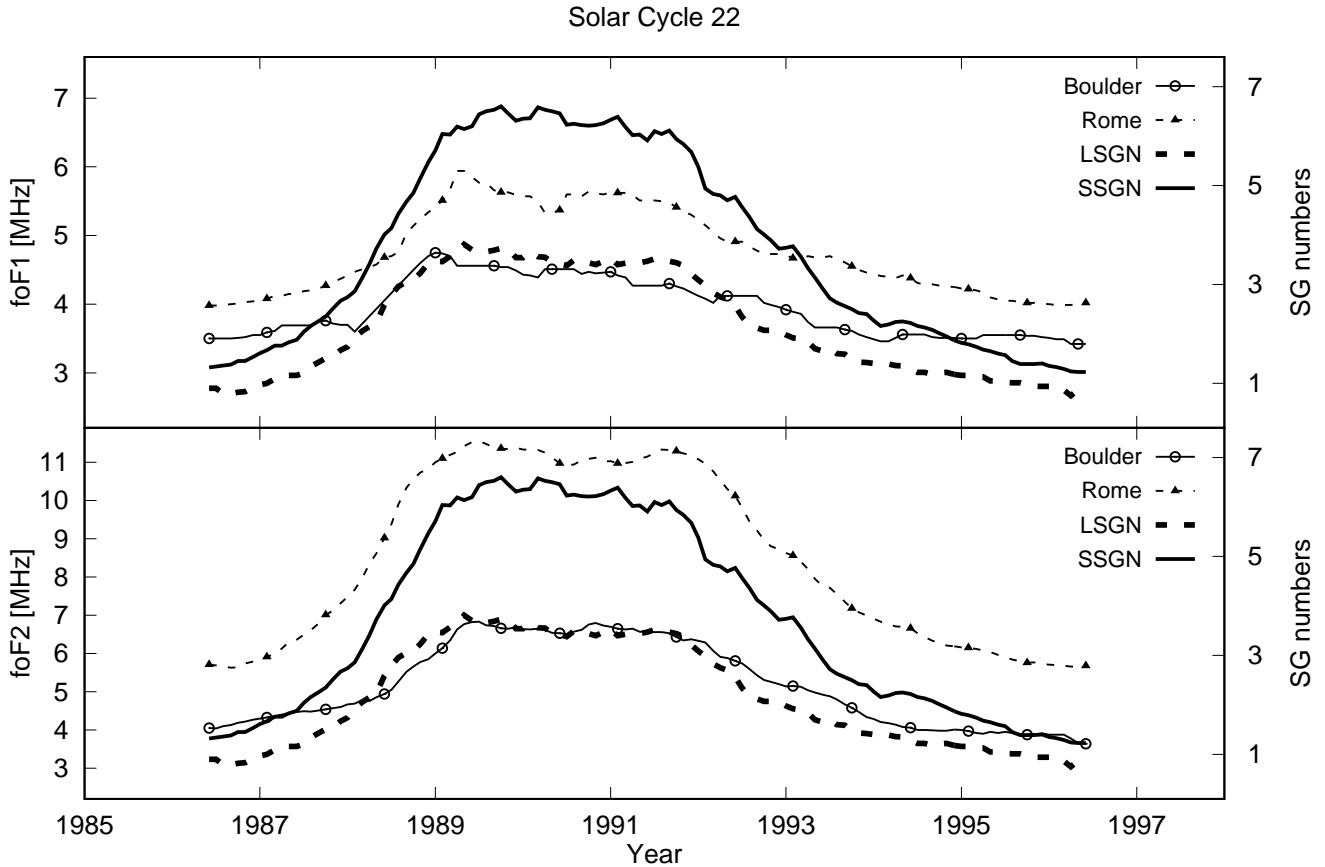


Figure 4. Same as Figure 3 but solar cycle 22.

cles (cycle 21, 22, and 23) and ascending and maximum phases of the solar cycle 24. Due to the lack of continuous station data our analysis could not cover all latitude intervals. Monthly median values calculated from data taken at 14:00 LT for each day of a given month for the investigated time period. In general, the f_0F_2 data have much better temporal coverage, while the number of total observing days strongly decreased during the winter times for the f_0F_1 data, as expected. But a few days of observation still exist. To calculate the monthly median values we used all existing data for each month. To remove the short term fluctuations due to gaps (especially in f_0F_1) in monthly median data and reveal the long term trend we used 12-step running average smoothing method. Three stations for cycle 21, two stations for cycle 22 and six stations for cycle 23 and 24 were analyzed because of the lack of continuous data.

3. ANALYSIS AND RESULTS

In this study, first, we compared temporal variation of SG numbers and ionospheric critical frequencies. Second we calculated Pearson correlation coefficients and their confidence levels between these data sets. For the confidence level Fisher's test which gives upper and lower bounds of correlation coefficients, were used. We used the highest error as an error level.

Figure 3 presents the temporal variations of the observed f_0F_1 (top panel), f_0F_2 (bottom panel), small

sunspot group numbers (SSGNs), and large sunspot group numbers (LSGNs) during the solar cycle 21. Thick solid and dashed lines denote the SSGNs and LSGNs, respectively. The other lines represent the different stations. Note that the SSGN and LSGN variations are overplotted in both the top and bottom panels to facilitate a better comparison with the critical frequencies. The subsequent Figures 4, 5, and 6 present the associated temporal variations for the solar cycles 22, 23, and 24, respectively, in a manner similar to Figure 3. Overall, we have a coverage approximately from 1976 to 2015. Analysis of the different solar cycle behavior of the both critical frequencies and the SG numbers suggest that SSGN and LSGN data show almost similar variations during the solar cycles except for solar cycle 23. The LSGN peaks about one to two years later than the SSGN during solar cycle 23, while both large and small SG numbers peak at almost the same time or the differences between two maxima are not such a prominent feature during solar cycles 21, 22, and 24. In general, f_0F_1 and f_0F_2 demonstrate different solar cycle variations compared with the variations of the SGs, which suggests that the different ionospheric regions are sensitive to the activity of the different regions in the solar photosphere.

Overall, in terms of temporal variations, the f_0F_1 follows the small SG numbers, while the f_0F_2 follows the large SG numbers. The marked difference between large

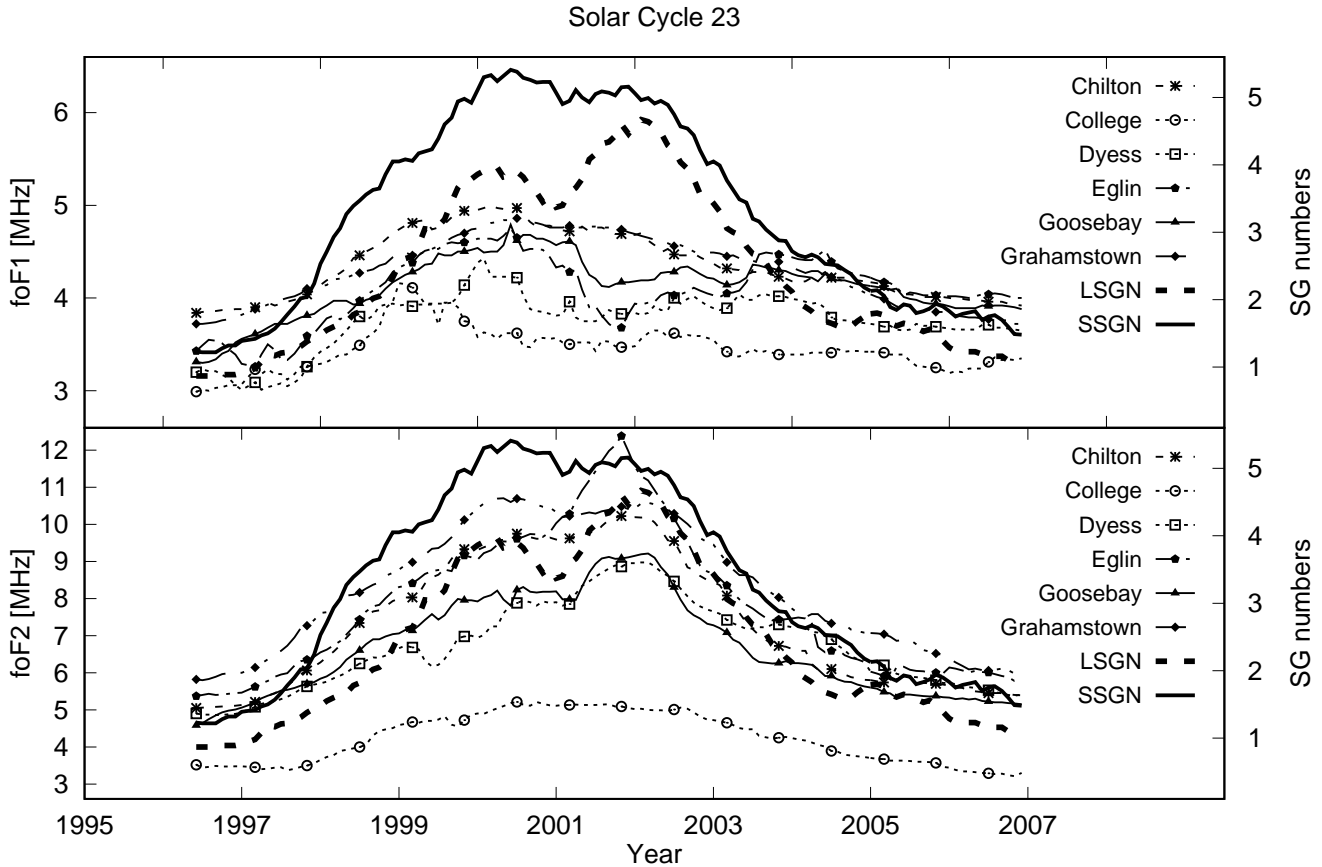


Figure 5. Same as Figure 3 but solar cycle 23.

and small SGs temporal behavior during a cycle is clearly seen during solar cycle 23 (Figure 5), during which the occurrence of the strong SSGN global maximum coincides with the LSGN local maximum in 2000 and the occurrence of the weak local maximum coincides with the LSGN global maximum in 2002, demonstrating the ~ 2 -year preceding of the peak SSGN with respect to the LSGN. In general, intercomparison of the critical frequency trends with the SG numbers suggest that the f_0F_2 data follows the large SG number variations, while the variations of f_0F_1 rather follow the small SG numbers. These findings are pronounced much more clearly in the solar cycle 23 (see Figures 2, 3, 4, and 5). However, during the other solar cycles, this effect is masked out because the LSGN and SSGN have similar temporal variations (there are no prominent differences between the two peaks) in terms of the timing of their global maxima. Overall, these results suggest that the ionospheric f_0F_1 and f_0F_2 critical frequencies respond differently to the different origin of the solar activity, characterized by the different sunspot groups. Essentially, most of the active events such as solar flares and CMEs occur in the large/complex active regions, mainly populated by large sunspots (Kilcik et al. 2011b). Thus our results, in particular related to the cycle 23, indicate that f_0F_2 , and thus the F_2 region, is sensitive to active sun (flares, CMEs), while the f_0F_1 , and thus the F_1 region, is sensi-

tive to quite sun (regular solar wind).

In Table 1 we presented correlation coefficients between 12-step running averaged SG numbers and ionospheric critical frequencies for each cycle, separately. As shown in this table, generally correlation coefficients between f_0F_1 and f_0F_2 critical frequencies and large and small SG numbers are comparable during all cycles except cycle 23. During solar cycle 23 large groups are well correlated with f_0F_2 , while small groups with f_0F_1 for most of the stations.

4. DISCUSSION AND CONCLUSIONS

The long-term temporal variations of the observed ionospheric f_0F_1 and f_0F_2 critical frequencies have been investigated for the last four solar cycles from the cycles 21 to 24 (1976 through 2015) and been compared with the associated variations of the solar activity represented by small (SSGNs) and large (LSGNs) sunspot group numbers. The same analysis may well have been carried out by other solar activity indicators such as TSI, $F_{10.7}$ etc., but it is known that their temporal variations were highly correlated by the sunspot number. We preferably have sought to place the emphasis on the importance of SG numbers due to their separability into small and large structures and thus their insightful physical association with coronal mass ejections (CMEs) and solar flare activity (Kilcik et al. 2017). Our key finding is that the temporal variations of the ionospheric critical frequen-

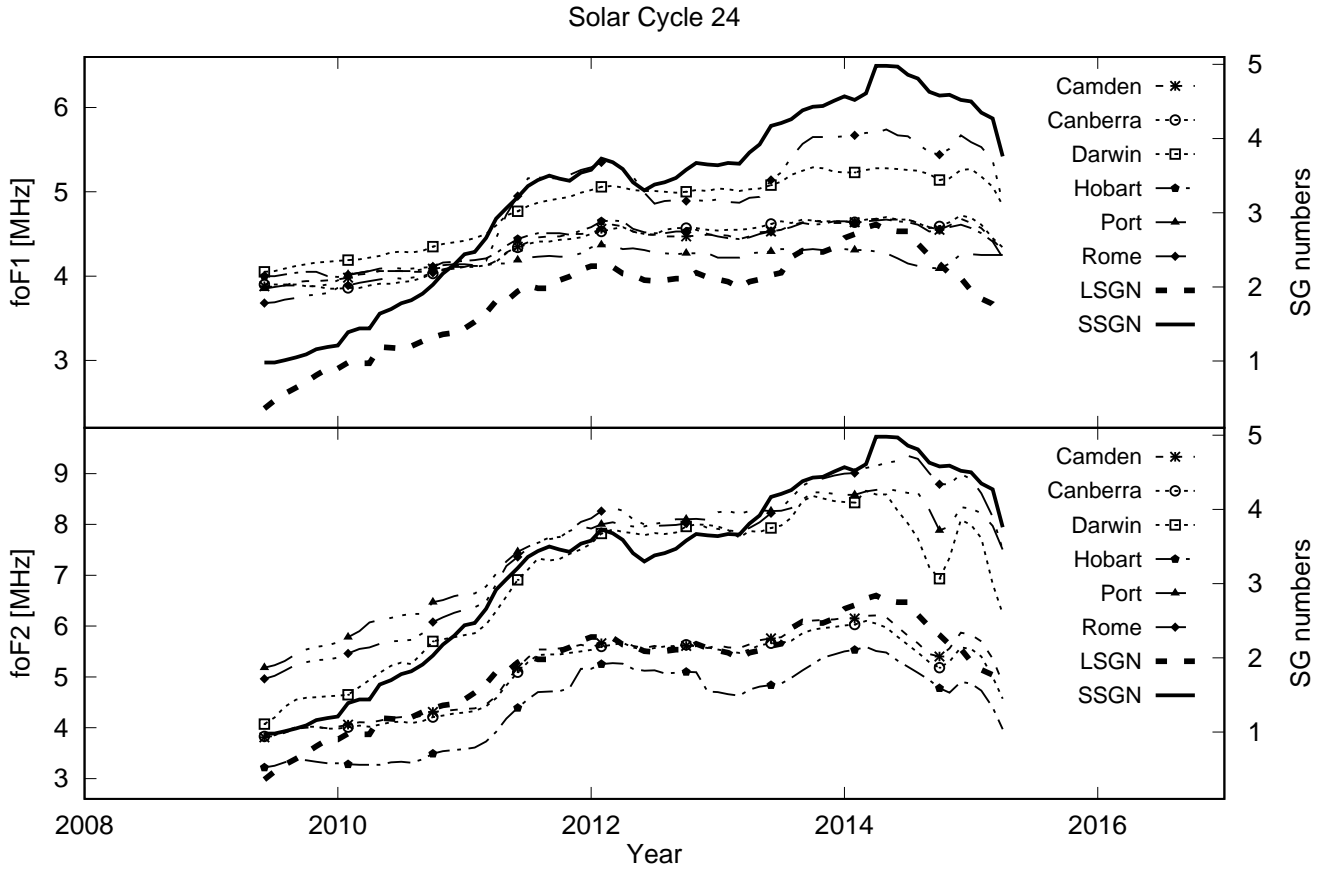


Figure 6. Same as Figure 3 but solar cycle 24.

cies exhibit different solar cycle variations in terms of the SSGN and LSGN for the investigated time periods, in particular during cycle 23 (1996 through 2008).

Close investigation of the solar cycle 23 demonstrates an anomalous character compared to the solar cycles 21, 22, and 24. Namely, the global maximum of the SSGN occurs about 2 years earlier than the global maximum of LSGN. Interestingly, the f_0F_1 peak occurs at the same time as the occurrence of the global maximum of SSGN, while the f_0F_2 peak occurs at the same as the global maximum of LSGN. This effects is not depictable in the other cycles as the SSGN and LSGN generally maximize at the same time.

The possible long-term drivers of F_1 and F_2 regions critical frequencies include long-term variations in solar and geomagnetic activity, various greenhouse gases (e.g., CO_2 , CH_4) concentrations, ozone variations, water vapor and the magnetic field variations (Yue et al. 2006; Mikhailov 2008; Laštovička et al. 2012; Gordiyenko et al. 2014, and references therein). Here we focused exclusively on the solar effects on the ionospheric critical frequencies.

There has been previous scientific evidence that the solar cycle 23 was indeed an anomalous cycle. For instance, de Toma et al. (2004) found that the magnitude of TSI during the solar cycle 23 was comparable to solar cycle 22, while the magnitude of the ISSN was much

lower. Kilcik et al. (2011a) found that the facular area was also lower during the solar cycle 23. Contrary to small groups, which were strongly diminished during solar cycle 23, the number of large groups were comparable to, or even higher, than that of solar cycle 22 (Lefevre and Clette 2011; Kilcik et al. 2011a, 2014). Also many low-latitude coronal holes observed during the declining phase of cycle 23 (see Abramenko et al. 2010). It can be also noted that Gordiyenko et al. (2014) found similar results for the annual means of f_0F_2 (see Figure 4 in their paper). On the other hand, it is known that all solar activity indicators such as the TSI, SSA, F10.7, etc., peaked in 2002 during solar cycle 23. Also, similar to the ISSN, they all show double/multiple peaks near the maximum of this cycle.

Kilcik et al. (2011a) investigated SG numbers in two categories, as large and small, from 1964 to 2008. They found that the number of large groups peaked about two years later than small ones except for solar cycle 22 (1986–1996): the difference between large and small SG numbers is very prominent during solar cycle 23, while maxima were almost flat during solar cycle 21 and 22. Recently, Kilcik et al. (2014) analyzed the sunspot counts (SSCs) in four categories, as small, medium, large and final, from 1982 to 2014, and found similar results for SSCs. Here, we analyzed monthly median f_0F_1 and f_0F_2 for 1976 - 2015 time interval which include this

Table 1

Correlation analysis results for each station and solar data set for the last four solar cycles. Errors are calculated by using Fisher test.

Station	foF1		foF2	
	LSGN	SSGN	LSGN	SSGN
<i>Solar Cycle 21</i>				
Boulder	0.94 ± 0.02	0.94 ± 0.02	0.97 ± 0.01	0.99 < 0.01
Hobart	0.96 ± 0.02	0.99 < 0.01	0.98 ± 0.01	0.99 < 0.01
Point	0.98 ± 0.01	0.94 ± 0.02	0.97 ± 0.01	0.99 < 0.01
<i>Solar Cycle 22</i>				
Boulder	0.97 ± 0.01	0.96 ± 0.02	0.97 ± 0.01	0.99 < 0.01
Rome	0.98 ± 0.01	0.98 ± 0.01	0.99 < 0.01	0.99 < 0.01
<i>Solar Cycle 23</i>				
Chilton	0.86 ± 0.05	0.96 ± 0.02	0.98 ± 0.01	0.99 < 0.01
College	0.61 ± 0.12	0.72 ± 0.10	0.95 ± 0.02	0.97 ± 0.01
Dyess	0.68 ± 0.11	0.71 ± 0.10	0.92 ± 0.03	0.86 ± 0.05
Eglin	0.44 ± 0.15	0.53 ± 0.14	0.96 ± 0.02	0.94 ± 0.02
Goosebay	0.75 ± 0.09	0.82 ± 0.07	0.97 ± 0.01	0.97 ± 0.01
Grahamstown	0.93 ± 0.03	0.98 ± 0.01	0.97 ± 0.01	0.99 < 0.01
<i>Solar Cycle 24</i>				
Camden	0.96 ± 0.02	0.97 ± 0.02	0.95 ± 0.03	0.95 ± 0.03
Canberra	0.94 ± 0.04	0.97 ± 0.02	0.95 ± 0.03	0.92 ± 0.05
Darwin	0.96 ± 0.02	0.98 ± 0.01	0.96 ± 0.02	0.94 ± 0.03
Hobart	0.96 ± 0.02	0.94 ± 0.03	0.95 ± 0.03	0.91 ± 0.05
Port	0.85 ± 0.08	0.80 ± 0.10	0.97 ± 0.02	0.97 ± 0.02
Rome	0.95 ± 0.03	0.97 ± 0.02	0.96 ± 0.02	0.98 ± 0.01

anomalous solar cycle 23 (1996–2008) and which clearly reveals that during solar cycle 23 the f_0F_1 is following the temporal variation of SSGN, while the f_0F_2 is following the LSGN. Both f_0F_1 and f_0F_2 have flat peaks during solar cycles 21 and 22 and they peaked in the second maximum of solar cycle 24 similar to SG numbers. Thus, our results for the anomalous solar cycle 23 along with its comparison with the cycles 21, 22, and 24 provide further insight into the effects of solar activity on the ionosphere. Specifically, they indicate that variations of the two different sunspot categories have different effect on these ionospheric layers: the first one is the geo-effective solar events (flares, CMEs, etc.) which are mainly produced by large/complex sunspot groups (Eren et al. 2017). They mostly describe the active sun and are more effective on the ionospheric F_2 layer critical frequency. The second one relating to the small SGs may produce quite rare flares compared to the large ones (Lee et al. 2012). These sunspot groups may describe the quite/weak solar activity.

The ionospheric F_1 and F_2 layers have different physical characteristics. F_1 layer is photochemically controlled and behaves like a Chapman layer, demonstrating overall a $\cos \chi$ (solar zenith angle) dependence, while the F_2 layer can substantially depart from a simple solar control due to the relative significance of dynamical processes. Also, the ionospheric F_2 layer is very susceptible to geomagnetic activity and CMEs (Burns et al. 2007). It is the most anomalous and variable, hence the least predictable ionospheric layer due to the complex interplay of chemistry, dynamics (e.g., diffusive transport), and coupling to electric fields of magnetospheric origin. Generally, the characteristics and intensity of CMEs and solar winds can be associated with the scales of the SGs, providing a link between the ionospheric F -region and the solar atmosphere. Thus, especially our analysis pertaining to cycle 23 lead to the conclusion that the long-term variations of the ionospheric F_2 layer is influenced more

by the variations of LSGNs, while the long-term variations of F_1 layer is linked more to the variations of the SSGNs. In other words, this implies that ionospheric F_2 layer is more sensitive to CMEs and fast solar winds (active sun conditions), while the F_1 layer is more sensitive to slow/regular solar wind (quite sun conditions).

The sunspot group data were taken from the National Geophysical Data Center (NGDC) web page. The f_0F_1 and f_0F_2 data sets were retrieved from the Space Physics Interactive Data Resource (SPIDR) web page. This study was supported by the Scientific and Technical Council of Turkey by the Project of 115F031. One of us (JPR) acknowledges the International Space Science Institute (ISSI) in Bern (Switzerland) for a “visitor scientist” grant. EY was partially funded by the NSF grant AGS 1452137.

REFERENCES

- Abramenko, V., V. Yurchyshyn, J. Linker, Z. Miki, J. Luhmann, and C. O. Lee (2010), Low-latitude coronal holes at the minimum of the 23rd solar cycle, *Astrophys. J.*, 712(2), 813.
- Burns, A.G., S. C. Solomon, W. Wang, and T. L. Killeen (2007), The ionospheric and thermospheric response to CMEs: Challenges and successes, *J. Atmos. Sol.-Terr. Phys.*, 69, 77–85, doi:10.1016/j.jastp.2006.06.010.
- Chakrabarty, D., B. G. Fejer, S. Gurubaran, T. K. Pant, M. A. Abdu, and R. Sekar (2014), On the pre-midnight ascent of f-layer in the june solstice during the deep solar minimum in 2008 over the indian sector, *J. Atmos. Sol.-Terr. Phys.*, 121, 177–187, doi:10.1016/j.astp.2014.01.002.
- Clette, F., L. Svalgaard, J. M. Vaquero, and E. W. Cliver (2014), Revisiting the sunspot number. a 400-year perspective on the solar cycle, *Space Sci. Rev.*, 186, 35–103.
- Cortie, A. (1901), On the types of sun-spot disturbances, *Astrophys. J.*, 13, 260–264, doi:10.1086/140816.
- de Toma, G., O. R. White, G. A. Chapman, S. R. Walton, D. G. Preminger, and A. M. Cookson (2004), Solar cycle 23: an anomalous cycle?, *Astrophys. J.*, 609, 1140–1152, doi:10.1086/421104.
- Elias, A. G., B. S. Zossi, E. Yiğit, Z. Saavedra, B. F. de Haro Barbas (2017), Earth’s magnetic field effect on MUF calculation and consequences for hmF2 trend estimates, *J. Atmos. Sol.-Terr. Phys.*, doi:10.1016/j.jastp.2017.03.004.

- Eren, S., A. Kilcik, T. Atay, R. Miteva, V. Yurchyshyn, J. P. Rozelot, and A. Ozguc (2017), Flare Production Potential Associated with Different Sunspot Groups, *Mont. Not. R. Ast. Soc.*, *465*, 68–75, doi:10.1093/mnras/stw2742
- Forbes, J. M., S. C. Palo, and X. Zhang (2000), Variability of the ionosphere, *J. Atmos. Sol.-Terr. Phys.*, *62*, 685–693, doi:10.1016/S1364-6826(00)00029-8.
- Gordiyenko, G. I., V. V. V. A. F. Yakovets, and Y. G. Litvinov (2014), A long-term trend in the f2-layer critical frequency as observed at alma-ata ionosonde station, *Earth Planets Space*, *66*, 125.
- Hathaway, D. H. (2015). The solar cycle. *Living Rev. Solar Phys.* *12* (4).
- Kane, R. (2006), Are the double-peaks in solar indices during solar maxima of cycle 23 reflected in ionospheric fof2?, *J. Atmos. Sol.-Terr. Phys.*, *68*, 877–880, doi:10.1016/j.asjp.2006.02.003.
- Kilcik, A., V. B. Yurchyshyn, V. Abramenko, P. Goode, N. Gopalswamy, A. Ozguc, and J. P. Rozelot (2011a), Maximum coronal mass ejection speed as an indicator of solar and geomagnetic activities, *The Astrophysical Journal*, *727*, 44–49, doi:10.1088/0004-637X/727/1/44.
- Kilcik, A., V. B. Yurchyshyn, V. Abramenko, P. Goode, A. Ozguc, J. P. Rozelot, and W. Cao (2011b), Time distribution of large and small sunspot groups over four solar cycles, *The Astrophysical Journal*, *730*, 30–37, doi:10.1088/0004-637X/730/1/30.
- Kilcik, A., V. B. Yurchyshyn, A. Ozguc, and J. P. Rozelot (2014), Solar cycle 24: Curious changes in the relative numbers of sunspot group types, *Astrophys. J. Letts.*, *794*, L2, doi:10.1088/2041-8205/794/1/L2.
- Kilcik, A., E. Yiğit, V. B. Yurchyshyn, A. Ozguc, and J. P. Rozelot (2017), Solar and Geomagnetic Activity Relation for the Last two Solar Cycles *Sun and Geosphere*, *12*, 31–39
- Laštovička, J., S. C. Solomon, and L. Qian (2012), Trends in the neutral and ionized upper atmosphere, *Space Sci. Rev.*, *168*, 113–145, doi:10.1007/s11214-011-9799-3.
- Lee, K., Y. J. Moon, J. Y. Lee, K. S. Lee, and H. Na (2012), Solar flare occurrence rate and probability in terms of the sunspot classification supplemented with sunspot area and its changes, *Solar Physics*, *281*, 639–650, doi:10.1007/s11207-012-0091-9.
- Lefevre, L., and F. A. Clette (2011), A global small sunspot deficit at the base of the index anomalies of solar cycle 23, *Astronomy and Astrophysics*, *536*, L11, doi:10.1051/0004-6361/201118034.
- McIntosh, P. S. (1990), The classification of sunspot groups, *Solar Phys.*, *125*(2), 251–267, doi:10.1007/BF00158405.
- Mikhailov, A. V. (2008), Ionospheric f1 layer long-term trends and the geomagnetic control concept, *Ann. Geophys.*, *26*, 3793–3803.
- Smithro, C. G., and J. J. Sojka (2005), Behaviour of the ionosphere and thermosphere subject extreme solar cycle conditions, *J. Geophys. Res.*, *110*, A08306, doi:10.1029/2004JA010782.
- Vaquero, J. M. (2007), Historical sunspot observations: A review, *Adv. Space Res.*, *40*, 929–941, doi:10.1016/j.asr.2007.01.087.
- Wolf, R. (1861). Abstract of his latest results. *Mon. Not. R. Astron. Soc.* *21*, 77.
- Yiğit, E., and A. S. Medvedev (2010), Internal gravity waves in the thermosphere during low and high solar activity: Simulation study., *J. Geophys. Res.*, *115*, A00G02, doi:10.1029/2009JA015106.
- Yiğit, E., and A. S. Medvedev (2015), Internal wave coupling processes in Earth's atmosphere, *Adv. Space Res.*, *55*, 983–1003, doi:10.1016/j.asr.2014.11.020.
- Yiğit, E., P. K. Knížová, K. Georgieva, and W. Ward (2016), A review of vertical coupling in the atmosphere-ionosphere system: Effects of waves, sudden stratospheric warmings, space weather, and of solar activity, *J. Atmos. Sol.-Terr. Phys.*, doi:10.1016/j.jastp.2016.02.011.
- Yue, X., W. Wan, L. Liu, B. Ning, and B. Zhao (2006), Applying artificial neural network to derive long-term fof2 trends in the asia/pacific sector from ionosonde observations, *J. Geophys. Res.*, *111*, A10,303, doi:10.1029/2005JA011577.